Supplementary Information for

Enantiodetermining processes in the synthesis of alanine, serine, and isovaline

Qingli Liao[1], Peng Xie[2], and Zhao Wang[1]

[1]School of Physical Science and Technology, Guangxi University, 530004 Nanning, China
[2]School of Chemistry and Chemical Engineering, Guangxi University, 530004 Nanning, China

I. Benchmark Calculations

We conducted benchmark calculations to determine the computed Gibbs free energy of the intermediates (IMs) and transition states (TSs) in two distinct pathways. The results obtained using our method, density functional theory (DFT) at the M06-2X/6-31+G(d,p) level, were compared with those obtained using three commonly used methods. These methods include DFT at the B3LYP/6-31+G(d,p) level, as well as Møller Plesset perturbation theory of second order (MP2) with 6-31+G(d,p) and aug-cc-pVDZ basis sets. The comparison results are presented in the table below.

Path A1	M06-2X 6-31+G(d,p)	B3LYP 6-31+G(d,p)	MP2 6-31+G(d,p)	MP2 aug-cc-pVDZ
TS1	14.5	10.4	14.5	15.9
TS2	5.1	3.6	8.4	8.0
TS3	16.1	14.3	19.7	19.8
TS4	−1.2	3.9	5.0	3.7
IM1	−6.8	−7.5	−9.1	−7.7
IM2	−11.0	−10.3	−16.1	−14.4
IM3	−32.0	−32.6	−33.1	−31.2
Path B1				
TS1	9.1	6.7	9.2	7.5
TS2	−9.1	−12.5	−13.2	−14.2
TS3	−8.6	−11.6	−3.6	−3.0
TS4	1.3	1.1	6.0	4.4
TS5	−21.2	−15.0	−15.0	−16.1
TS6	−4.2	−5.5	−6.1	−8.4
TS7	−15.0	−14.1	−16.5	−19.6
TS8	−12.3	−10.1	−12.2	−14.9
IM1	−30.6	−30.6	−41.1	−41.4
IM2	−16.5	−17.4	−26.3	−24.6
IM3	−38.3	−37.2	−35.4	−34.6
IM4	−45.5	−45.2	−41.4	−41.1
IM5	−55.8	−56.4	−56.1	−56.2
IM6	−54.1	−54.5	−53.0	−52.9
IM7	−14.7	−15.8	−15.9	−16.7

Table 1: Computed Gibbs free energies (in kcal/mol) of the IMs and TSs in Path A1 and B1. Comparison between results obtained by using four different methods.

II. Reaction Dynamics

To access the feasibility of the proposed reactions in interstellar medium (ISM), we have computed the reaction rate coefficient k and the half-life time of reactants $t_{1/2}$ as a function of temperature T based on ΔG of the proposed pathways, using the transition state theory developed by Eyring (J. Chem. Phys., 1935, 3, 107–115),

$$t_{1/2} = \frac{ln2}{k} = \frac{h}{C\kappa_B T} e^{\frac{\Delta G}{RT}} ln2 \tag{1}$$

where C is the transmission coefficient, κ_B the Boltzmann constant, T the absolute temperature, h the Planck constant, and R the molar gas constant. C is assumed to be 1 as an approximation, assuming that tunneling effects can be neglected (Zamirri et al., 2019). This approximation is in general less valid for lower barriers, especially at low temperature. We note that at low interstellar temperatures, and for not too high and wide barriers, quantum tunneling may play a prominent role favoring reaction rates (Kayanuma et al., 2017). The use of semiclassical approaches (with, for example, the Eckart formula (Miller, 1975)) or the instanton theory (Richardson, 2016) may, in general, be more appropriate in such a case.

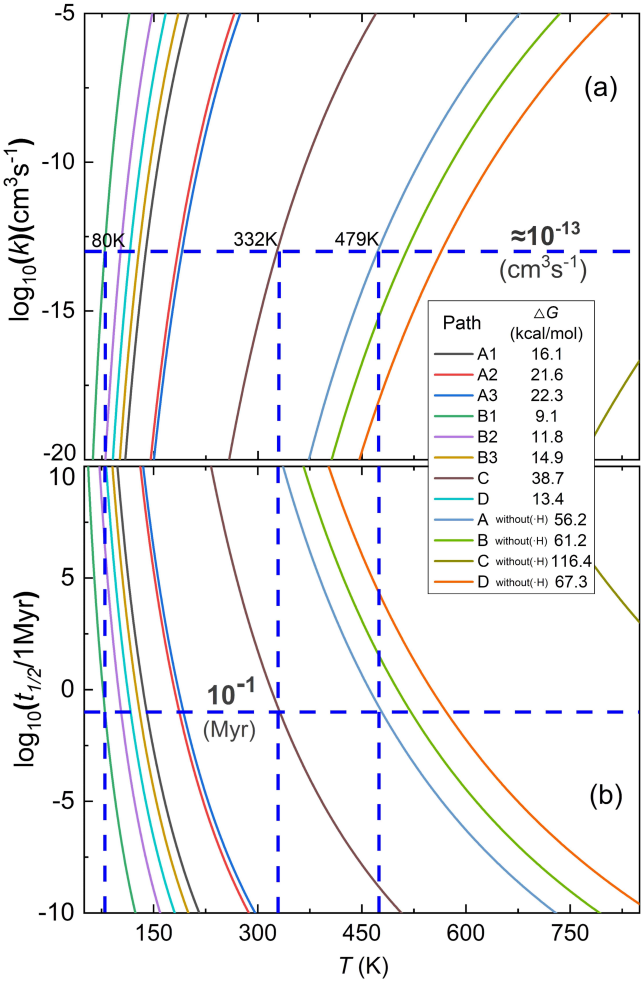

Figure 1. (a) Reaction rate coefficient k and (b) half-life time $t_{1/2}$ vs temperature for different barriers of the optimal pathways in the studied reactions.

The results show that, for achieving a half-life time shorter than 10^5 years (intersections of dashed lines in the lower panel), the temperature needs to be above 80, 332, and 479 K (intersections of dashed lines in the upper panel). This roughly corresponds to a rate coefficient greater than 10^{-13}cm^{3}s^{-1} (above the horizontal dashed line in the upper panel). We note that the catalyzed reactions reported here are three-body collision processes, which are often considered impossible in the ISM due to the rate dependence not only on the reactant concentration but also on the catalyst's concentration. However, this is not the case for the ·H-catalyzed reaction, as the. ·H's

concentration greatly exceeds that of the reactants. The here-considered ternary reactions are thus effectively pseudo-binary reactions.

III. Molecular Orbital Analysis

In order to explain why the barrier of Reaction B is lower than that of Reaction A, we show the molecular orbitals of the key intermediates (IMs) during the rate-determining step in the optimal pathways (A1 and B1) of these two reactions in Figure 2. According to the frontier molecular orbital theory, the success of a molecular reaction is related to the conservation of orbital symmetry before and after the reaction. The incompatibility of the lowest unoccupied molecular orbital (LUMO, right) of $CH_3CH(NH_2)OH$ and the highest occupied molecular orbital (HOMO, left) of $\cdot CHO$ in Reaction A, as highlighted in the red dashed frame in the upper panel, can hinder the reaction. In contrast, the molecular orbital symmetry between the IMs of Reaction B is more coherent, as seen in the lower panel. This is further evidenced by the HOMO-LUMO energy gap of between the IMs of the reaction A being 7.2 kcal/mol, while that of the reaction B is only 0.4 kcal/mol.

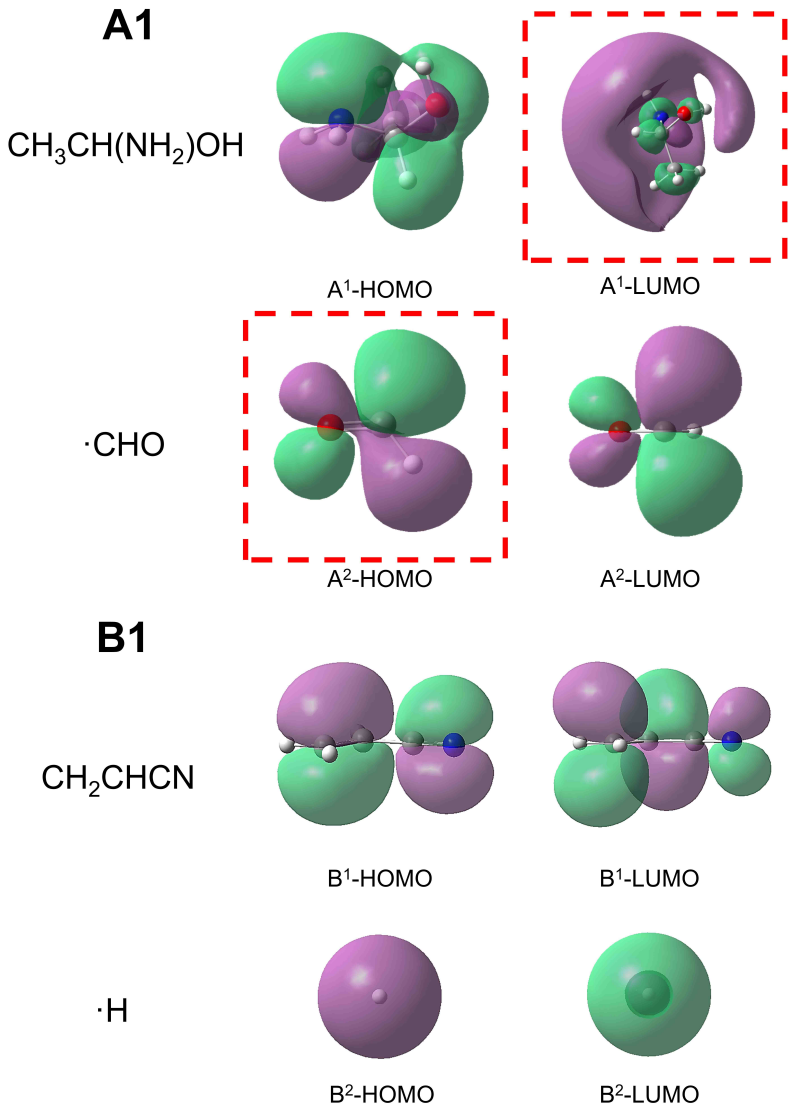

Figure 2. HOMO (left) and LUMO (right) of $CH_3CH(NH_2)OH$, $\cdot CHO$, CH_2CHCN and $\cdot H$.

IV. Other Optimal Pathways to Ala

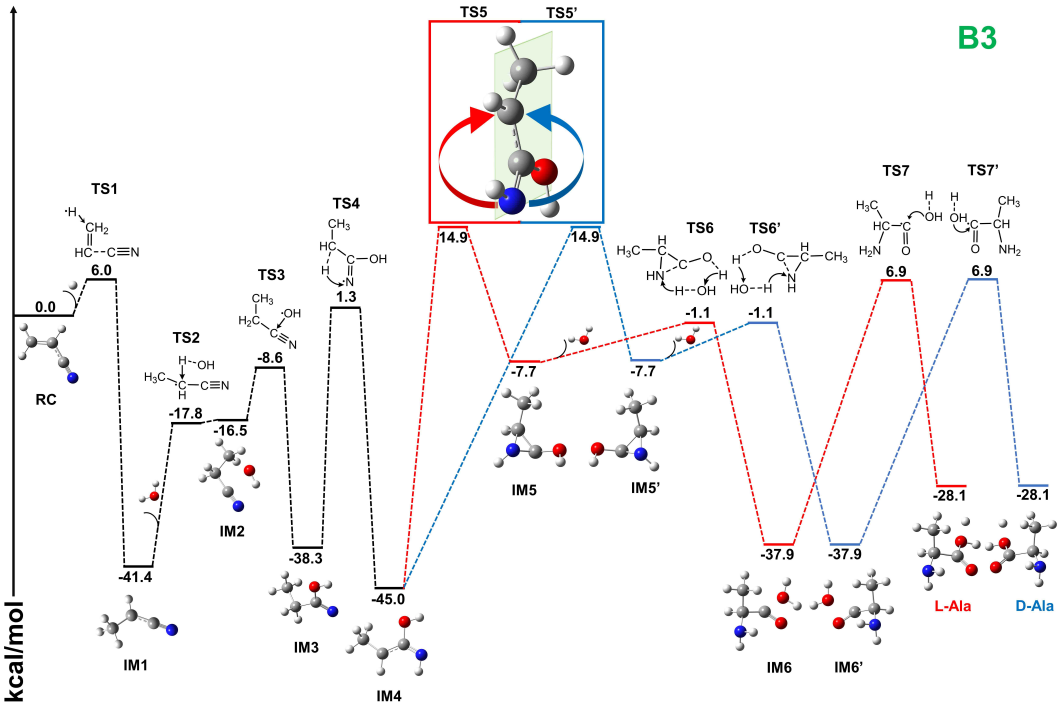

Figure 3. Potential diagram of Pathway B3.

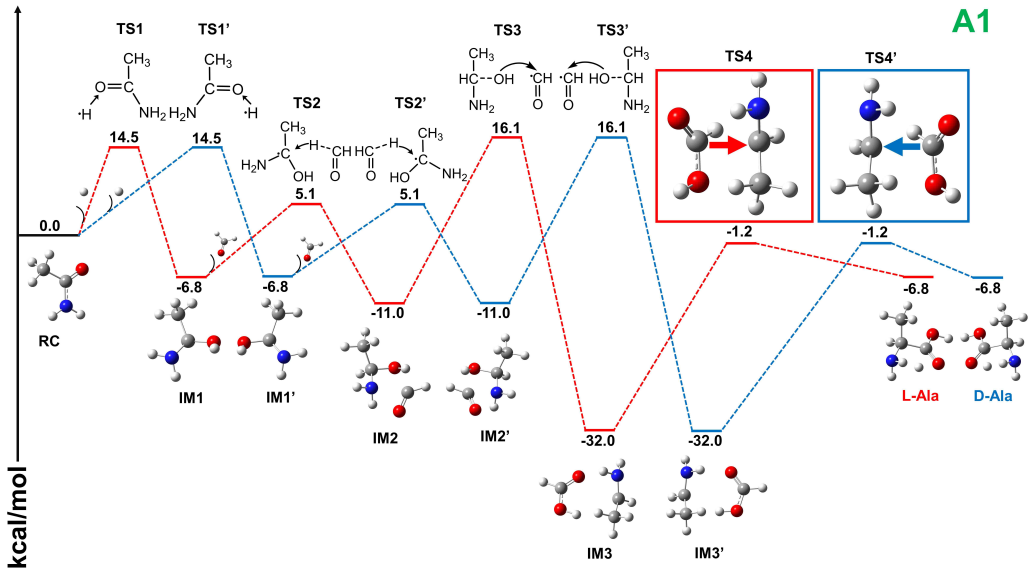

Figure 4. Potential diagram of Pathway A1.

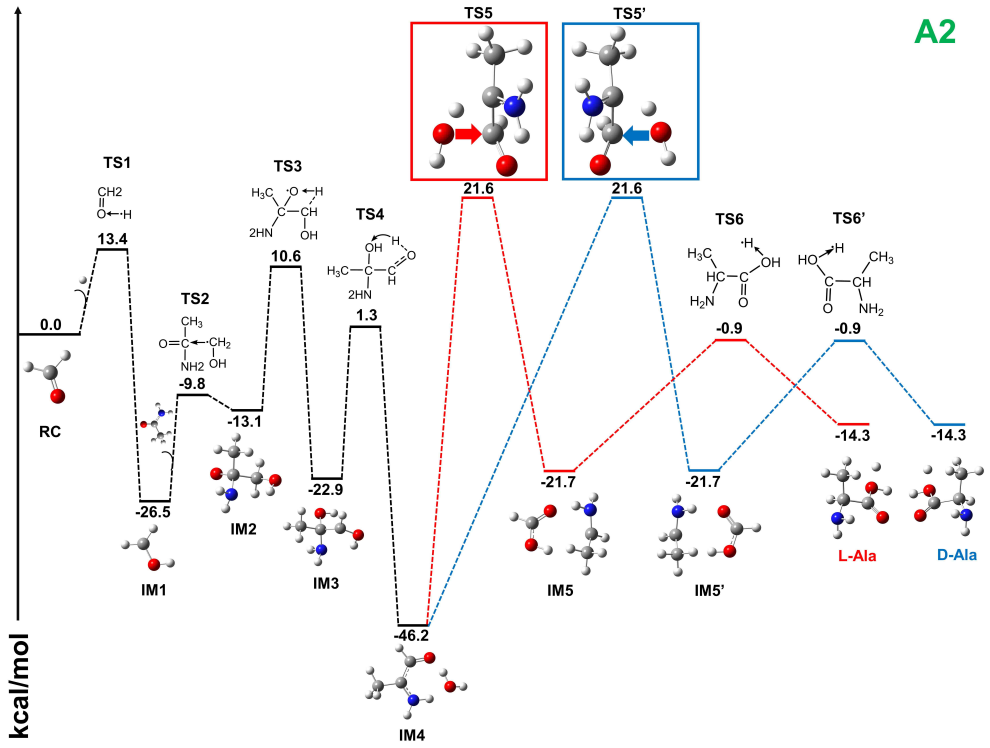

Figure 5. Potential diagram of Pathway A2.

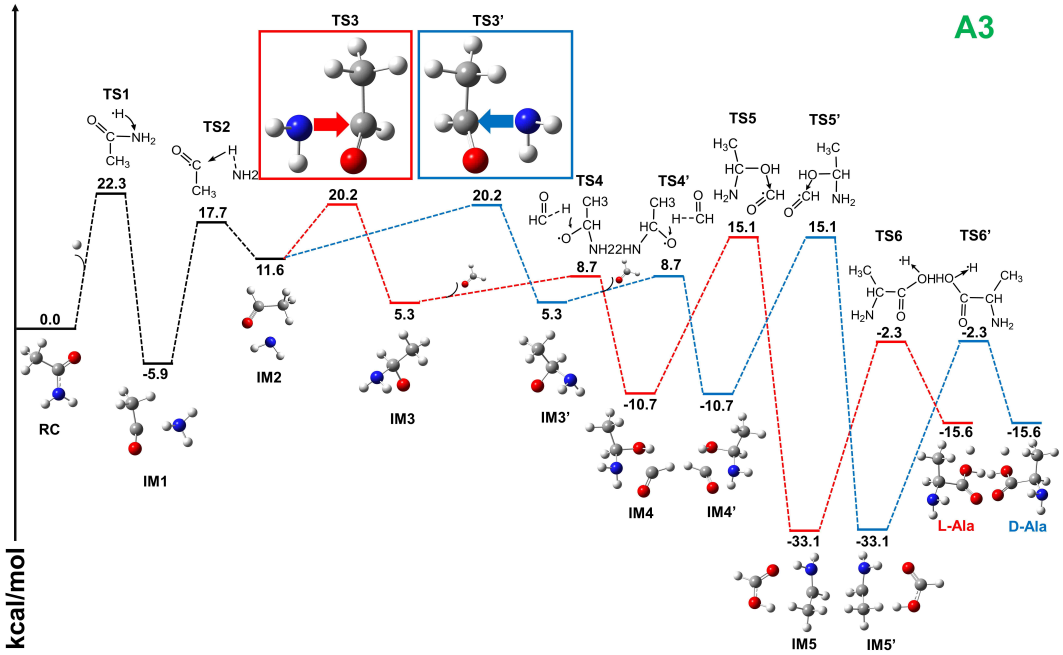

Figure 6. Potential diagram of Pathway A3.

V. Rotation Potential of a "Single" Bond

The figure presented below depicts the energy profile required for rotating the central C-C bond in $CH_3CNH_2C_2H_5$ (IM4 in Pathway D), as a function of the rotation angle. The rotation is performed relative to the axis of the bond under consideration.

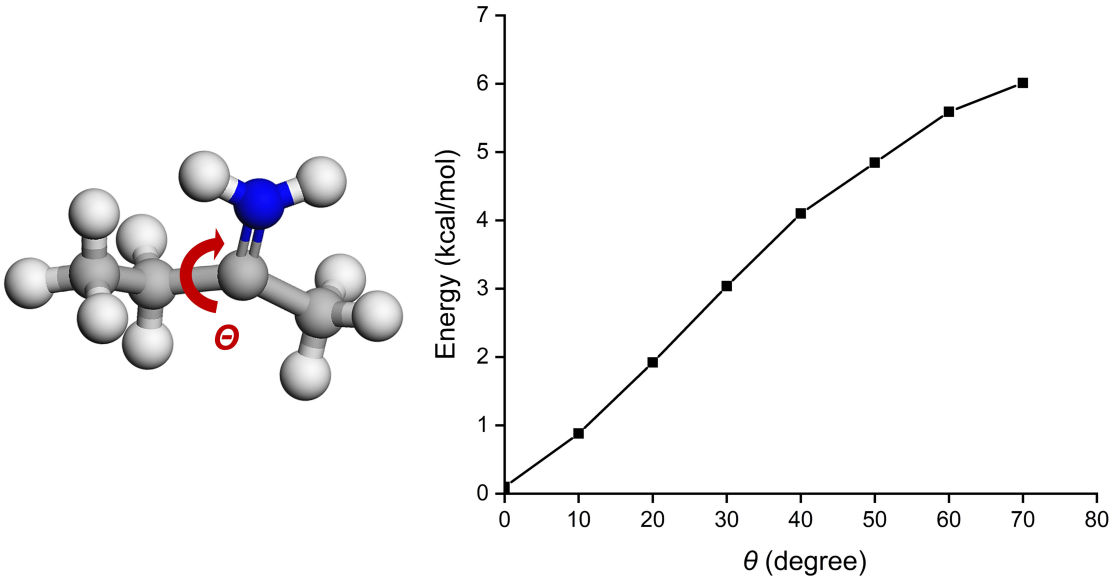

Figure 7. Gibbs free energy vs the rotation angle for the central C-C bond in $CH_3CNH_2C_2H_5$.

VI. Alternative path for Reaction D

We present an alternative three-body reaction for the sythesis of Isovaline:

$$CH_3CHNH + C_2H_4 + HCOOH \longrightarrow C_5H_{11}NO_2 \quad \text{(D, Isov)}.$$

Here ethanimine (CH_3CHNH) and formic acid (HCOOH) were detected towards Sgr B2 (Loomis et al., 2013; Zuckerman et al., 1971), and C_2H_4 was detected in IRC+10216 as "hot" molecules with characteristic rotation temperature > 400 K (Betz, 1981). This reaction begins with the collision of CH_3CHNH and $\cdot H$ (TS1), which leads to the formation of CH_3CNH and H_2 (IM1) when $\cdot H$ takes a H atom from the central C site of CH_3CHNH. Next, C_2H_4 reacts with CH_3CNH to produce $CH_3CNHC_2H_4$ (IM2). Finally, H_2 collides with the CH_2 group of IM2, yielding $CH_3CNHC_2H_5$ and a $\cdot H$ radical (IM3).

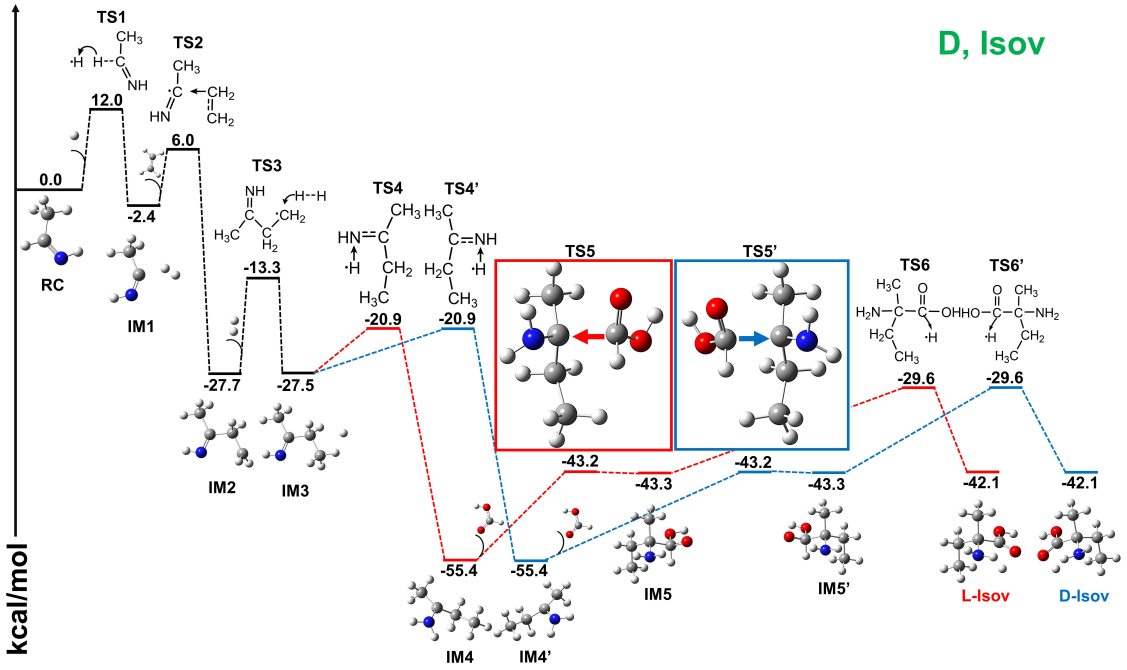

Figure 8. Potential diagram of the optimal pathway of Reaction D towards Isov.

In the following step, $\cdot H$ generated in the previous step reacted with the N site in $CH_3CNHC_2H_5$, producing $CH_3CNH_2C_2H_5$ (IM4/IM4') that has no chirality center. Then, the addition of a HCOOH group to IM4/IM4' produced a chirality center at the central C site, resulting in $C_5H_{12}NO_2$ (IM5/IM5'). At first glance, it may appear that the enantiomer is determined in this step by the different directions in which the HCOOH is added, as indicated by the arrows in Figure 8. However, the optimal collision direction is actually dictated by the configurations of IM4/IM4'. IM4/IM4 exhibit mirror symmetry and cannot be superimposed through rotation, similar to the case of IM6/IM6' in Figure 4. It is important to note that although IM4 and IM4' have a C atom connected to four groups, it does not meet the definition of a chirality center. Consequently, the enantioselection occurs from IM3 to IM4/IM4', rather than in the subsequent step where the chirality center is created.

VII. Energy values and vibrational frequencies

In the attached file Data.zip, we provide the energy values without the Gibbs correction (in Energy.csv) and the vibrational frequencies (in Frequency.csv) of the intermediates for all the proposed reaction paths.

References

Betz, A. L. 1981, Astrophys. J., 244, L103
Kayanuma, M., Kidachi, K., Shoji, M., et al. 2017, Chem. Phys. Lett., 687, 178
Loomis, R. A., Zaleski, D. P., Steber, A. L., et al. 2013, Astrophys. J., 765, L9
Miller, W. H. 1975, J. Chem. Phys., 62, 1899
Richardson, J. O. 2016, J. Chem. Phys., 144, 114106
Zamirri, L., Ugliengo, P., Ceccarelli, C., & Rimola, A. 2019, ACS Earth Space Chem., 3, 1499
Zuckerman, B., Ball, J. A., & Gottlieb, C. A. 1971, Astrophys. J., 163, L41